58

The Journal of the Astronautical Sciences, Vol. 44, No. 2, April-June 1996, pp. 129–147

Gravity Gradient Gyroscope Drifts in the NASA Relativity Mission/Gravity Probe B Experiment

N. Jeremy Kasdin[1] and Christian Gauthier[2]

Abstract

This paper examines the torques and resulting drift of the Relativity Mission or Gravity Probe B (GP-B) gyroscopes due to gravity gradient forces. Drifts are examined for both forces transmitted through the gyroscope suspension and torques due to the gravity gradient acting directly on the spherical rotor. The orbit averaged gravity gradients torques are derived considering a nonspherical Earth (J_2 oblateness only) and a slightly eccentric orbit. The effects of the Sun and Moon on the gyroscopes are also discussed. The resulting drift rates for various guide star candidates is presented.

Introduction

The Relativity Mission, or Gravity Probe B (GP-B), is a NASA experiment to test Einstein's General Theory of Relativity. In 1959, Leonard Schiff of the Stanford University Physics Department predicted, using General Relativity, that a local, free-falling inertial frame in a polar orbit about the spinning Earth would undergo two orthogonal rotations with respect to the universe's inertial (fixed) frame. Schiff's predictions, called the Geodetic and Frame dragging effects, are represented by the angular velocity $\boldsymbol{\Omega}_T$ expressed as

$$\boldsymbol{\Omega}_T = \underbrace{\frac{3GM_\oplus}{2c^2r^3}(\mathbf{r}\times\mathbf{v})}_{\text{Geodetic}} + \underbrace{\frac{GI_\oplus}{c^2r^3}\left[\frac{3}{r^2}(\boldsymbol{\omega}_\oplus\cdot\mathbf{r})\mathbf{r} - \boldsymbol{\omega}_\oplus\right]}_{\text{Frame Dragging}} \tag{1}$$

where c is the speed of light, $\mathbf{r}$ is the radius of the orbit, $\mathbf{v}$ is the velocity in orbit, G is the universal gravitation constant, $M_\oplus$ is the mass of the Earth, $I_\oplus$ is the polar moment of inertia of the Earth, and $\boldsymbol{\omega}_\oplus$ is the angular velocity of the Earth.

[1]Chief Systems Engineer Gravity Probe B, W. W. Hansen Experimental Physics Laboratory, Stanford University, Stanford, CA 94305-4085.
[2]Member of the Loran NELS Steering Committee, DCN Ingenierie, 8 Bvd Victor, Paris, France.

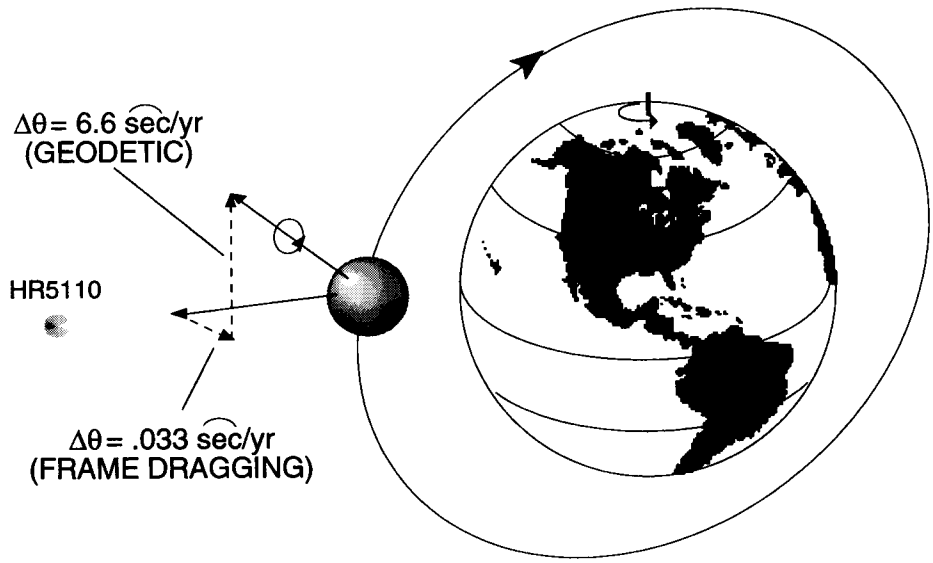

FIG. 1. The Relativity Experiment.

These drifts, depicted in Fig. 1, are not predicted by Newton's gravity theory and amount to 6.6 arcsec/year in the orbit plane (the *geodetic* effect) and 33 milliarcsec/year perpendicular to the orbit plane (the *frame-dragging* effect) for a 650 km altitude polar orbit. Schiff proposed that these effects be measured by orbiting near perfect gyroscopes and comparing their spin axis directions (fixed in the local, free-falling frame) with a far inertial reference provided by pointing an onboard telescope at a fixed guide star [1, 2].

Gravity Probe B is the culmination of this proposal [3–10]. Scheduled to be launched in 1999, the GP-B science instrument consists of four superconducting, electrostatically suspended gyroscopes (Fig. 2) housed in a block of fused quartz that is optically contacted to a quartz telescope, used to point the satellite at the guide star (Fig. 3). In order to obtain an uncorrupted measure of the relativistic effects, it is necessary to free the gyroscope's quartz rotors from all inertially fixed forces and torques, thus reducing the Newtonian drift below the experiment goal of 0.3 milliarcsec/year.

There are two categories of these disturbances—torques arising from interactions between the imperfections in the electrostatic suspension system and asphericities in the rotor (known as support-dependent torques) and torques arising from direct action of conservative and nonconservative forces acting on the rotor (known as support-independent torques). In order to minimize the effects of support induced torques, accelerations of the satellite causing the suspension system to act are virtually eliminated by the use of drag free control [11]. This system maintains near zero acceleration by controlling the satellite to fly centered about a proof mass (which is thus in a purely gravitational orbit or *geodesic*) to nanometer position accuracy and thus reducing the accelerations on the gyroscopes to under 10^{-8} g. Note also that the satellite is rolling about the line-of-sight to the guide star. This acts to both average many body fixed torques on the gyroscopes

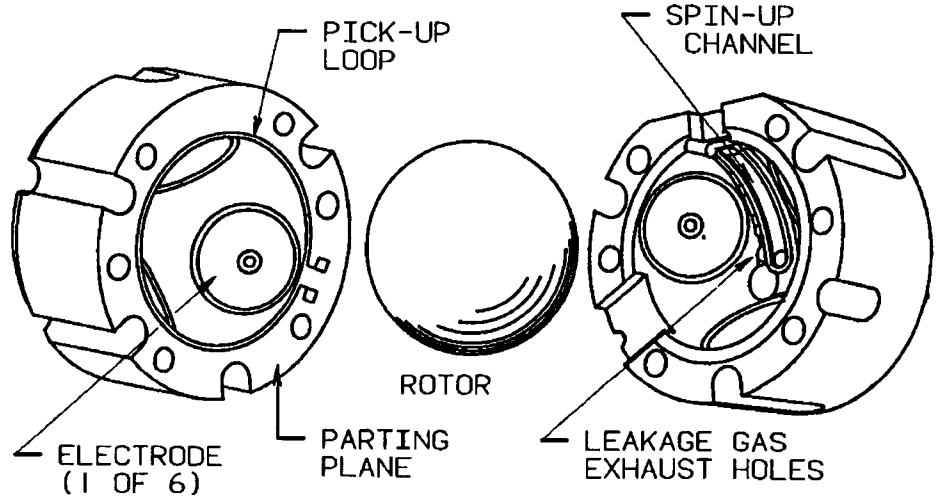

FIG. 2. The Gravity Probe B Gyroscope.

and shift the measurement signal away from zero frequency where the readout sensors are less stable.

The largest torques acting on the gyroscope arise from disturbances due to gradients in the Earth's gravity field. These torques fall under both the support-dependent and support-independent category. The support-dependent torques occur because the gyroscopes are a distance from the proof mass and thus experience a gravity gradient force. This force must be supported against by the

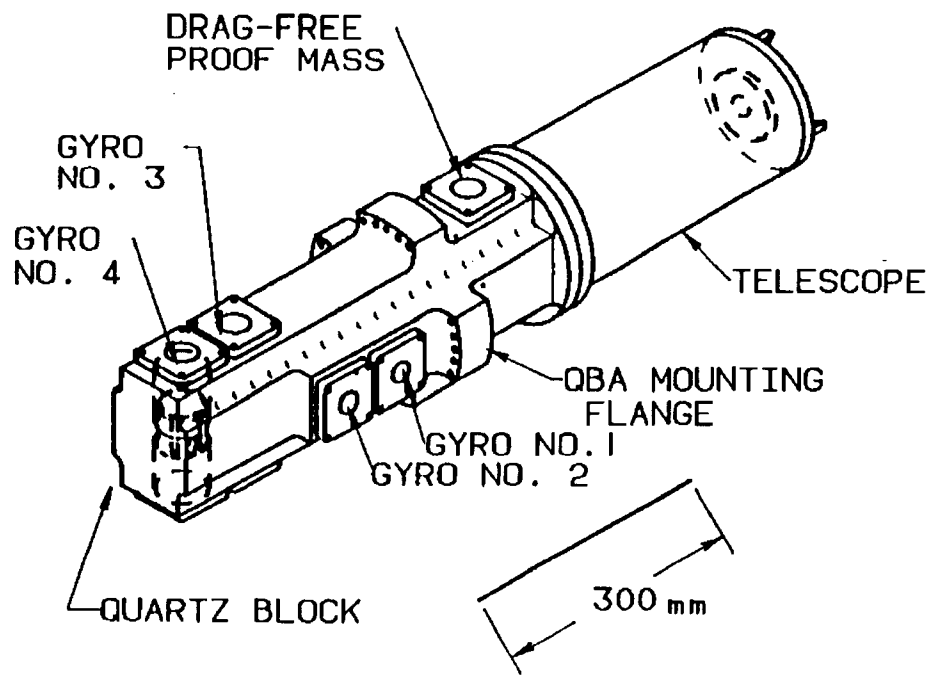

FIG. 3. The Quartz Block Assembly and Telescope.

suspension system which also produces unwanted small gyroscope torques. The support-independent torques occur because the slightly non-isoinertial rotors (that is, rotors with non-equal principal moments-of-inertia) interact with the gradient of the gravity field directly. (The normalized inertia differences, $\Delta I/I$, are on the order of 10^{-6} to 10^{-5}.)

Using the work of Keiser [12] that modeled the gyroscope torques induced by the electrostatic suspension, Vassar [13] and Vassar et al. [14] computed the support induced gravity gradient torques on the gyroscope for a perfectly circular orbit about a spherical earth. They showed that the torque on the gyroscope is proportional to the angular deviation between the satellite line-of-sight and the orbit plane, which can be written as a function of the orbit co-inclination (i'), node (Ω) and guide star declination (δ):

$$\tau \propto i' \sin \delta + \Omega \cos \delta \tag{2}$$

where i' and Ω are assumed first order small (very near polar orbit) and Ω is defined as the angle of the line of nodes from the guide star direction rather than the Vernal Equinox. Equation (2) implies that for an ideal circular, polar orbit, gravity gradient torques average to zero. An additional benefit of such an orbit is that the two relativistic effects are exactly orthogonal [14, 15], whereas for small deviations of the coinclination and node the larger geodetic effect corrupts the frame dragging measurement. This can be seen by looking at the drift rate of the gyroscope due to relativity (equation (1)) for small co-inclination and node resolved in the inertial 1 and 2 directions (North and East) [15]:

$$\begin{aligned} \Omega_G &= A_G(i' \cos \delta - \Omega \sin \delta)\hat{\mathbf{E}} + A_G\hat{\mathbf{N}} \\ \Omega_{FD} &= A_{FD} \cos \delta \, \hat{\mathbf{E}} - A_{FD} 3i' \cos \delta \, \hat{\mathbf{N}} \end{aligned} \tag{3}$$

where A_G and A_{FD} are the geodetic and frame dragging drift rates from equation (1):

$$A_G = \frac{3}{2} \frac{\mu_e n}{c^2 a(1 - e_o^2)}, \qquad A_{FD} = \frac{GI_\oplus \omega_\oplus}{2c^2 a^3 (1 - e_o^2)^{3/2}} \tag{4}$$

Axelrad et al. [15] recognized that such an ideal orbit is impossible in practice. The various effects of the Earth's shape, Sun, Moon, and tides, for example, will cause deviations of the orbit plane away from these nominal conditions. The object is then to find an initial target orbit such that the long term deviations over the year long experiment result in minimum average drift on the gyroscope. Axelrad et al. thus produced a simulation of the long term effects of the Earth oblateness, Sun, Moon, and tides and derived optimal target orbits and injection requirements for the GP-B spacecraft. Such orbits can be found for any of the possible GP-B guide stars.

This paper addresses the fact that the gyroscope drift equation derived by Vassar and used by Axelrad et al. only assumed a spherical Earth and circular orbit while the orbit modeling considered the more extensive perturbations mentioned. New torque and drift equations are thus derived considering the Earth's oblateness (J_2) and orbit eccentricity. The small effects of the Sun and Moon on the gyroscopes

are also examined. New drift mechanisms are shown proportional to J_2 while the drifts are shown to be independent (to first order) of orbit eccentricity.

In order to find these torques, first the satellite orbit is modeled including the J_2 oblateness perturbation. Then, the gravity force on the gyroscope is computed, including the J_2 effect as well as the direct gravity gradient. These are then used in the gyroscope torque equations, averaged over a satellite orbit, and finally inserted in the drift equations for the orbit averaged gyroscope drift.

Spacecraft Orbit Modeling

The first step in the calculation is to find accurate equations describing the satellite orbit defined by the free falling proof mass. Figure 4 shows a schematic of the GP-B satellite orbit. The vector $\mathbf{r}_p$ locating the proof mass is defined by its magnitude and argument of latitude ν.

While the orbit is nominally circular at a constant rate, the J_2 oblateness of the Earth introduces small perturbations. This nominal orbit is circular with radius r_0 and true anomaly θ. The position of the proof mass is then expressed:

$$\mathbf{r}_p(\nu) = (r_o + \delta r)\mathbf{u}_r(\theta) + r_o\delta\theta\ \mathbf{u}_\theta(\theta) \tag{5}$$

where $\mathbf{u}_r$ and $\mathbf{u}_\theta$ are unit vectors in the radial and tangential directions. The mean orbit rate is given by:

$$\dot{\theta} = n = \sqrt{\frac{\mu_e}{r_o^3}}\left[1 - \frac{3}{8}J_2\left(\frac{R_e}{r_o}\right)^2\right] \tag{6}$$

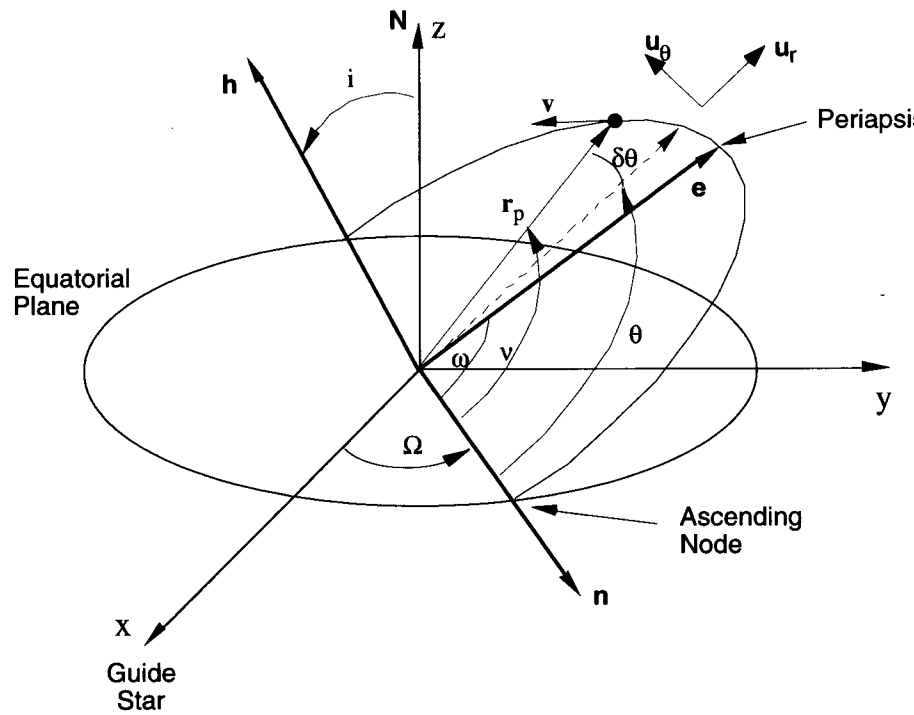

FIG. 4. The Satellite Orbit.

while the perturbations due to the oblateness (J_2) as derived by Breakwell [16] are:

$$\delta r = r_o\left[\frac{1}{4}J_2\left(\frac{R_e}{r_o}\right)^2 \cos(2\theta) - e_o\cos(\theta - \omega)\right]$$

$$\delta\theta = \frac{1}{8}J_2\left(\frac{R_e}{r_o}\right)^2 \sin(2\theta) + 2e_o\sin(\theta - \omega) \tag{7}$$

Note that the orbit modifications due to higher harmonics (J_3 and greater) are small compared to those caused by oblateness.

The final result is that the position can be expressed by the following equations:

$$\mathbf{r}_p(\nu) = r_p(\nu)\,\mathbf{u}_r(\nu) \tag{8}$$

$$r_p(\nu) \approx r_o + \delta r(\theta)$$

$$\nu \approx \theta + \delta\theta(\theta) \tag{9}$$

In the derivations that follow it will also prove useful to rotate from the inertial frame defined by the axes labeled x, y, and z in Fig. 4 to a frame in the plane of the orbit. This is accomplished by the following direction cosine matrix (assuming first order small i' and Ω):

$${}^{\text{orbit}}C^I = \begin{bmatrix} \cos\delta & -i' & \sin\delta \\ i'\cos\delta - \Omega\sin\delta & 1 & \Omega\cos\delta + i'\sin\delta \\ -\sin\delta & -\Omega & \cos\delta \end{bmatrix} \tag{10}$$

Therefore, the unit vector along $\mathbf{r}_p$ in the orbit frame is:

$$\mathbf{i}_{r_p}^{\text{orbit}} = \begin{bmatrix} \sin\nu \\ 0 \\ \cos\nu \end{bmatrix} \tag{11}$$

while rotated into the inertial frame it is given by:

$$\mathbf{i}_{r_p}^I = \begin{bmatrix} \cos\delta\sin\nu - \sin\delta\cos\nu \\ -i'\sin\nu - \Omega\cos\nu \\ \sin\delta\sin\nu + \cos\delta\cos\nu \end{bmatrix} \tag{12}$$

Note that throughout this paper a superscript I on a vector indicates that the vector is to be coordinated in the inertial frame. The absence of any superscript implies that the vector is coordinatized in the spacecraft body frame with z-axis along the telescope boresight (and roll axis), x-axis perpendicular to one of the gyroscope readout planes and y-axis completing the right hand set.

Gyroscope Equations

The first step in computing the gyroscope drift is to derive the rotational equations of motion for the gyroscope rotor. This is done by equating the inertial time derivative of the rotor angular momentum $\mathbf{L}$ with the torques on the rotor, $\boldsymbol{\tau}$, expressed in inertial space:

$$\left(\frac{d\mathbf{L}}{dt}\right)^I = \boldsymbol{\tau}^I \tag{13}$$

This equation is most easily completed by expressing $\mathbf{L}$ in a frame aligned with the spin axis of the rotor, $\boldsymbol{\omega}_s$, and taking the derivative there using the rotation angles of this frame with respect to inertial space, EW and NS. Note that the nominal orientation of the spin axis with respect to the inertial frame is aligned with the z-direction, i.e., the initial direction to the guide star (see Fig. 5). The relativistic effects are measured as a rotation of the angles NS (geodetic) and EW (frame dragging). Any additional drift due to Newtonian torques is an error indistinguishable from science (except to the extent it may have a unique time signature). The final equations of motion, linearized in the small angles EW and NS, are given by:

$$\begin{aligned} \dot{EW} &= -\frac{\tau_z^I}{L} EW - \frac{\tau_y^I}{L} \\ \dot{NS} &= -\frac{\tau_z^I}{L} NS + \frac{\tau_x^I}{L} \\ \dot{\Delta L} &= \tau_z^I + \tau_x^I NS - \tau_y^I EW \end{aligned} \tag{14}$$

The next section briefly discusses the derivation of the torques to be used in equation (14).

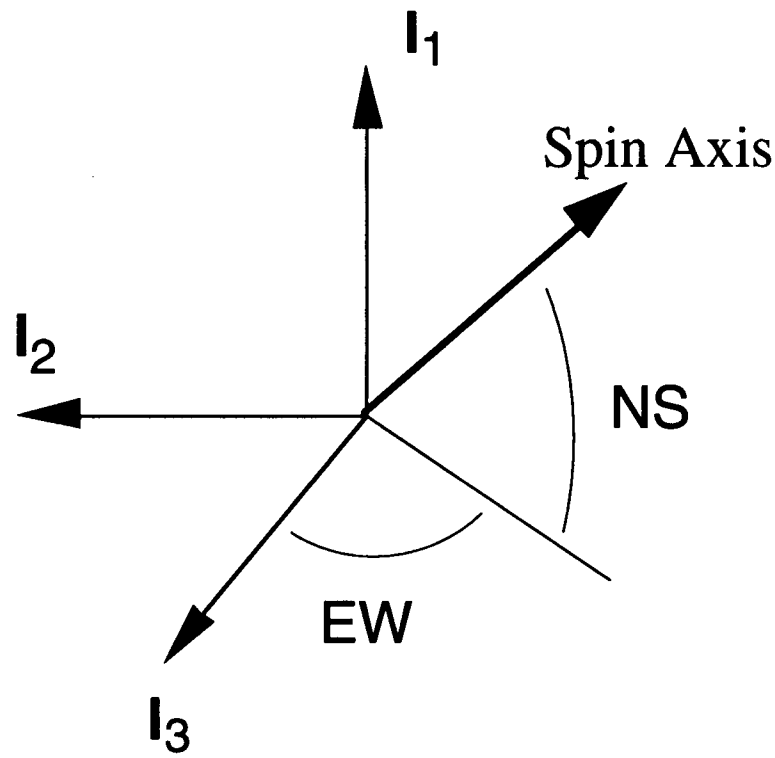

FIG. 5. The Spin Axis Direction in the Inertial Frame.

Gyroscope Suspension Torques

Once the drift equations of motion are derived, the task is to find expressions for the various torques on the gyroscope rotors. This has been an ongoing effort at Gravity Probe B in order to confirm the required 10^{-11} deg/hr performance of the gyroscopes. In this paper we focus on only one, though the largest, source of torque—that resulting from the Earth's gravity gradient. There are two sources of gravity gradient torques, direct torques acting on the inertia differences of the spherical rotors and indirect gravity gradient forces acting through the electrostatic suspension. This section provides a general description of the electrostatic torques on the rotor while the following section specifically derives the gravity gradient torques including orbit eccentricity and J_2 oblateness. Subsequently, the direct torques are addressed.

As mentioned earlier, the GP-B satellite is drag free, that is, it is forced to fly about a free floating proof mass that is in a purely gravitational orbit. This effectively cancels the drag on the satellite (within the bandwidth of the controller) and keeps the satellite in as ideal an inertial frame as possible. However, since the gyroscopes are not free floating, they must be suspended against residual motion of the spacecraft and excess gravity gradient forces. This is accomplished through a six electrode electrostatic suspension system depicted in Fig. 6. Unfortunately, because the gyroscope is not perfectly round, the electrostatic suspension forces used to center the rotor also result in small torques.

The first major effort to derive expressions for the electrostatic torques on the GP-B rotors was done by Keiser [12]. This has been followed since by a number of additional studies using his same method. His approach was to expand the rotor

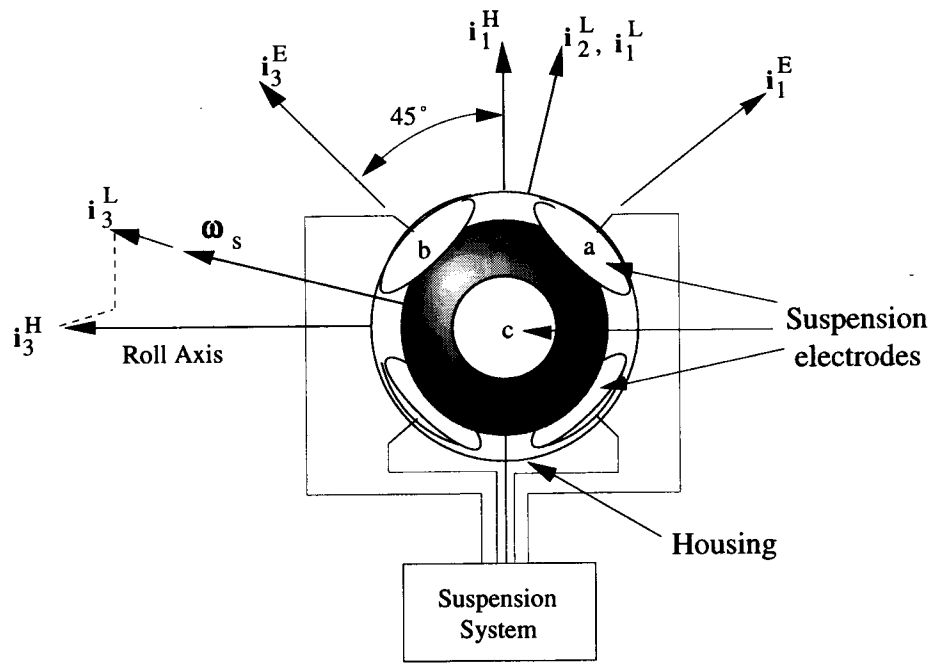

FIG. 6. Schematic of Rotor and Suspension Electrodes with Important Reference Frames: Housing (H); Electrode (E); and Spin Axis (L).

shape in a series of spherical harmonics and differentiate the total energy stored in the capacitance between the electrodes and rotor with respect to the rotation angle, η, about some arbitrary axis:

$$\tau_\eta = -\frac{\partial U}{\partial \eta} = -\frac{\partial U}{\partial C}\frac{\partial C}{\partial \eta} \tag{15}$$

where U is the total energy and C is the capacitance between the rotor and electrodes.

The second term on the right in equation (15) is a function of only geometry and can be found, with some work, in terms of the rotor shape coefficients in a spherical harmonic expansion and some dimensionless numbers. The final result is a set of equations for the torques on the rotor in terms of the rotor shape coefficients, r_{l0}, the roll angle of the satellite, ϕ, and the voltages on the top and bottom of the electrodes a, b, and c $(V_{a+}, V_{a-}, V_{b+}, V_{b-}, V_{c+}, V_{c-})$:

$$\begin{aligned}\tau_x^l = \frac{1}{2}\frac{\varepsilon_o r_g^2}{d_o^2}\Big\{ & -(V_{a+}^2 + V_{a-}^2 - V_{b+}^2 - V_{b-}^2)\sum_{l_{\text{even}}} A_1(l) r_{l0} \sin\phi \\ & - (V_{a+}^2 - V_{a-}^2 - V_{b+}^2 + V_{b-}^2) \\ & \times \sum_{l_{\text{odd}}} r_{l0}[A_2(l)\,(NS \sin 2\phi + EW \cos 2\phi) + A_0(l) EW] \\ & + (V_{a+}^2 - V_{a-}^2 + V_{b+}^2 - V_{b-}^2)\sum_{l_{\text{odd}}} A_1(l) r_{l0} \sin\phi \\ & + (V_{a+}^2 + V_{a-}^2 + V_{b+}^2 + V_{b-}^2) \\ & \times \sum_{l_{\text{even}}} r_{l0}[A_2(l)\,(NS \sin 2\phi + EW \cos 2\phi) + A_0(l) EW] \\ & - (V_{c+}^2 + V_{c-}^2) \\ & \times \sum_{l_{\text{even}}} r_{l0}[C_2(l)\,(NS \sin 2\phi + EW \cos 2\phi) - C_0(l) EW] \\ & - (V_{c+}^2 - V_{c-}^2)\sum_{l_{\text{odd}}} C_1(l) r_{l0} \cos\phi \Big\}\end{aligned} \tag{16a}$$

$$\begin{aligned}\tau_y^l = \frac{1}{2}\frac{\varepsilon_o r_g^2}{d_o^2}\Big\{ & (V_{a+}^2 + V_{a-}^2 - V_{b+}^2 - V_{b-}^2)\sum_{l_{\text{even}}} A_1(l) r_{l0} \cos\phi \\ & + (V_{a+}^2 - V_{a-}^2 - V_{b+}^2 + V_{b-}^2) \\ & \times \sum_{l_{\text{odd}}} r_{l0}[A_2(l)\,(-EW \sin 2\phi + NS \cos 2\phi) - A_0(l) NS] \\ & - (V_{a+}^2 - V_{a-}^2 + V_{b+}^2 - V_{b-}^2)\sum_{l_{\text{odd}}} A_1(l) r_{l0} \cos\phi \\ & - (V_{a+}^2 + V_{a-}^2 + V_{b+}^2 + V_{b-}^2) \\ & \times \sum_{l_{\text{even}}} r_{l0}[A_2(l)\,(-EW \sin 2\phi + NS \cos 2\phi) - A_0(l) NS]\end{aligned}$$

$$+ (V_{c+}^2 + V_{c-}^2)$$
$$\times \sum_{l_{\text{even}}} r_{l0}[C_2(l)(-EW \sin 2\phi + NS \cos 2\phi) + C_0(l)NS]$$
$$- (V_{c+}^2 - V_{c-}^2) \sum_{l_{\text{odd}}} C_1(l) r_{l0} \sin \phi \Bigg\} \tag{16b}$$

where A_0, A_1, A_2, C_0, C_1, and C_2 are dimensionless coefficients defined by DiDonna [17] and are of order one, d_o is the rotor/electrode gap (32 μm), r_g is the rotor radius, ε_o is the permitivity of free space, and ϕ is the roll angle of the satellite.

The voltages can be replaced by assuming a perfect suspension controller that exactly cancels the applied specific forces on the rotors, f_x, f_y, and f_z. The voltage differences are then given by:

$$V_{a+}^2 - V_{a-}^2 = \frac{2md_o^2}{\varepsilon_o \pi r_g^2 \sin^2 \theta_h}\left(\frac{f_x - f_z}{\sqrt{2}}\right)$$
$$V_{b+}^2 - V_{b-}^2 = \frac{2md_o^2}{\varepsilon_o \pi r_g^2 \sin^2 \theta_h}\left(\frac{f_x + f_z}{\sqrt{2}}\right)$$
$$V_{c+}^2 - V_{c-}^2 = -\frac{2md_o^2}{\varepsilon_o \pi r_g^2 \sin^2 \theta_h} f_y \tag{17}$$

where θ_h is the half angle of the electrode (29 degrees) and m is the rotor mass (roughly 65 g).

The voltage sums are slightly more difficult to find and require assumptions about the suspension implementation. For this work we have assumed the traditional preload based controller used on GP-B. In this, the nonlinear force equations (equation (17)) are linearized by adding and subtracting from the top and bottom electrode voltages a preload voltage of fixed amplitude, V_p. This is equivalent to a preload acceleration on the rotor from each electrode, h, for flight conditions of 2×10^{-7} g. The result is an expression for the sums of voltages:

$$V_{a+}^2 + V_{a-}^2 = \frac{2md_o^2}{\varepsilon_o \pi r_g^2 \sin^2 \theta_h}\left(h_a + \frac{(f_x - f_z)^2}{2h}\right)$$
$$V_{b+}^2 + V_{b-}^2 = \frac{2md_o^2}{\varepsilon_o \pi r_g^2 \sin^2 \theta_h}\left(h_b + \frac{(f_x + f_z)^2}{2h}\right)$$
$$V_{c+}^2 + V_{c-}^2 = \frac{2md_o^2}{\varepsilon_o \pi r_g^2 \sin^2 \theta_h}\left(h_c + \frac{f_y^2}{h}\right) \tag{18}$$

These voltage expressions are substituted into the torque equations to produce torques that depend upon the forces and preload on the rotor as well as its shape. They are divided up into odd terms, that is, those that depend only upon the odd coefficients of the rotor shape, and even terms, that is, those that depend only

upon even coefficients of rotor shape as follows:

$$(\tau_x^I)_{\text{odd}} = \frac{\sqrt{2}}{\pi s^2 \theta_h}\left\{ f_z \sum_{\text{odd}} r_{l0}[A_2(l)\,(NS\sin 2\phi + EW\cos 2\phi) + A_0(l)EW] + f_x \sum_{\text{odd}} r_{l0}A_1(l)\sin\phi + \frac{f_y}{\sqrt{2}} \sum_{\text{odd}} r_{l0}C_1(l)\cos\phi \right\} \tag{19a}$$

$$(\tau_y^I)_{\text{odd}} = \frac{\sqrt{2}}{\pi s^2 \theta_h}\left\{ -f_z \sum_{\text{odd}} r_{l0}[A_2(l)\,(-EW\sin 2\phi + NS\cos 2\phi) - A_0(l)NS] - f_x \sum_{\text{odd}} r_{l0}A_1(l)\cos\phi + \frac{f_y}{\sqrt{2}} \sum_{\text{odd}} r_{l0}C_1(l)\sin\phi \right\} \tag{19b}$$

$$(\tau_x^I)_{\text{even}} = \frac{1}{\pi \sin^2\theta_h}\left\{ 2\frac{f_x f_z}{h} \sum_{\text{even}} r_{l0}A_1(l)\sin\phi + \frac{f_x^2 + f_y^2}{h} \sum_{\text{even}} r_{l0}[A_2(l)\,(NS\sin 2\phi + EW\cos 2\phi) + A_0(l)EW] - \frac{f_y^2}{h} \sum_{\text{even}} r_{l0}[C_2(l)\,(NS\sin 2\phi + EW\cos 2\phi) - C_0(l)EW] \right\} \tag{20a}$$

$$(\tau_y^I)_{\text{even}} = \frac{1}{\pi \sin^2\theta_h}\left\{ -2\frac{f_x f_z}{h} \sum_{\text{even}} r_{l0}A_1(l)\cos\phi - \frac{f_x^2 + f_y^2}{h} \sum_{\text{even}} r_{l0}[A_2(l)\,(-EW\sin 2\phi + NS\cos 2\phi) - A_0(l)NS] - \frac{f_y^2}{h} \sum_{\text{even}} r_{l0}[C_2(l)\,(-EW\sin 2\phi + NS\cos 2\phi) + C_0(l)NS] \right\} \tag{20b}$$

where here the torques have been normalized by the gyroscope mass. Observe that the preload dependence has been removed as that has no bearing on the gravity gradient induced torques.

Note that the odd terms depend upon the specific forces directly while the even terms depend upon the square of the voltages. It turns out that the dominant forces are given by the $l = 1$ terms (mass unbalance of the rotor) and $l = 2$ terms (rotor oblateness, primarily induced by the spin of the rotor), which simplifies the torque expressions significantly. In terms of the mass unbalance along the spin axis, z_s, the odd torque is given by:

$$\begin{aligned} (\tau_x^I)_1 &= -z_s\{f_2^I + f_3^I EW\} \\ (\tau_y^I)_1 &= z_s\{f_1^I - f_3^I NS\} \end{aligned} \tag{21}$$

where we have here expressed the specific forces applied by the suspension in the inertial frame for convenience. In terms of Δr, the difference between equatorial and polar radius of the rotor, the even oblateness torque is given by:

$$(\tau_x^I)_2 = \frac{-\Delta r \cos\theta_h}{h}\left\{\left(f_y^2 - \frac{(f_x^2 + f_z^2)}{2}\right)(NS \sin 2\phi + EW \cos 2\phi + EW) - 2f_x f_z \sin\phi\right\}$$

$$(\tau_y^I)_2 = \frac{-\Delta r \cos\theta_h}{h}\left\{\left(f_y^2 - \frac{(f_x^2 + f_z^2)}{2}\right)(EW \sin 2\phi - NS \cos 2\phi + NS) + 2f_x f_z \cos\phi\right\} \tag{22}$$

The largest contributor to these support induced torques comes from the suspension force used to center the rotor against the gravity gradient arising from the rotors not being located at the proof mass, that is, the nominal orbit location. These forces and resulting torques are described in the next section.

Gravity Gradient Support Induced Drift

As mentioned earlier, Vassar [18] computed the gravity gradient force on the gyroscope rotors and the resulting even and odd torques for a perfectly circular orbit about a spherical Earth. Axelrad et al. [15] then used this in their orbit simulations to find the optimal target orbit, considering variations in node and co-inclination, to minimize the final gyroscope drift. For a gyroscope located a distance $\mathbf{d}$ from the proof mass, the gravity gradient force for a spherical Earth is found from the standard formula:

$$\begin{aligned}\mathbf{F}_{gg} &= -\frac{\mu_e}{r_p^3(1+\alpha)^{3/2}}\left\{\mathbf{d} + \left[1 - (1+\alpha)^{3/2}\right]\mathbf{r}_p\right\} \\ &= -\frac{\mu_e}{r_p^3(1+\alpha)^{3/2}}\left[\mathbf{d} - g(\alpha)\mathbf{r}_p\right]\end{aligned} \tag{23}$$

where $\alpha = (d^2 + 2\mathbf{r}_p \cdot \mathbf{d})/r_p^2$.

The function $g(\alpha)$ can be given by Battin's formula:

$$g(\alpha) = (1+\alpha)^{3/2} - 1 = \frac{\alpha(3 + 3\alpha + \alpha^2)}{1 + (1+\alpha)^{3/2}} \tag{24}$$

For the GP-B case where the distance from the proof mass to gyroscope is very small compared to the orbit radius, the gravity gradient force can be linearized with little error in the small quantity (d/r_p):

$$\mathbf{F}_{gg} \approx -n^2 d[\mathbf{i}_d - 3(\mathbf{i}_{r_p} \cdot \mathbf{i}_d)\mathbf{i}_{r_p}] \tag{25}$$

where n is the nominal orbit rate $\sqrt{\mu_e/r_p^3}$, $\mathbf{i}_d$ is the unit vector along $\mathbf{d}$, and $\mathbf{i}_{r_p}$ is the unit vector along $\mathbf{r}_p$. When equation (25) is computed for a nominally polar

orbit aligned with the guide star, the result, linearized in i' (the co-inclination) and Ω (the right ascension relative to the guide star) and averaged over the orbit is:

$$(\mathbf{F}^I_{gg})_{\text{average}} = n^2 d \begin{bmatrix} 0 \\ (3/2)(i' \sin\delta + \Omega\cos\delta) \\ -1/2 \end{bmatrix} \tag{26}$$

where δ is the declination of the guide star. This is the result found by Vassar and results in the torque dependence given by equation (2). In the next section, the gravity gradient torque expression is modified to include the effects of the Earth's oblateness (J_2), small eccentricity (e_o), Sun, and Moon effects in order to be more consistent with the orbit modeling and to search for possible modifications of the optimal target orbit.

Specific Gravity Gradient with Oblateness and Eccentricity

The gravity gradient force on the rotor is modified by an additional small term when considering the oblateness of the Earth:

$$\mathbf{F} = \mathbf{F}_{gg} + \mathbf{f}_{gg} \tag{27}$$

where the second term is found by considering the gradient of the total gravitational force including oblateness and ignoring the smaller higher order terms:

$$\mathbf{F}_g = -\frac{\mu_e}{r^3}\mathbf{r} - \frac{1}{2}\frac{\mu_e}{r^3}J_2\left(\frac{R_e}{r}\right)^2\left[6(\mathbf{r}\cdot\mathbf{N})\mathbf{N} + 3\mathbf{r} - 15\left(\frac{\mathbf{r}\cdot\mathbf{N}}{r}\right)^2\mathbf{r}\right] \tag{28}$$

where $\mathbf{N}$ is the unit vector directed along the Earth's spin axis.

This operation results in the expression for the small gravity gradient force due to J_2:

$$\mathbf{f}_{gg} = -\frac{1}{2}\frac{\mu_e}{r_p^3(1+\alpha)^{5/2}}J_2\left(\frac{R_e}{r_p}\right)^2\Bigg\{6(\mathbf{d}\cdot\mathbf{N})\mathbf{N} + 3\mathbf{d} - h(\alpha)[6(\mathbf{r}_p\cdot\mathbf{N})\mathbf{N} + 3\mathbf{r}_p] + \frac{15g(\alpha)}{(1+\alpha)}(\mathbf{i}_{r_p}\cdot\mathbf{N})^2\mathbf{r}_p - 15(\mathbf{i}_{r_p}\cdot\mathbf{N})^2\frac{\mathbf{d}}{(1+\alpha)} - \left[15\left(\frac{\mathbf{d}\cdot\mathbf{N}}{r_p}\right)^2 + 30(\mathbf{i}_{r_p}\cdot\mathbf{N})\left(\frac{\mathbf{d}\cdot\mathbf{N}}{r_p}\right)\right]\frac{\mathbf{d}+\mathbf{r}_p}{(1+\alpha)}\Bigg\} \tag{29}$$

where $h(\alpha) = (1+\alpha)^{5/2} - 1$.

This expression can also be linearized in the small quantity (d/r_p) with little error; the resulting first order expression for the gravity gradient force is:

$$\mathbf{f}_{gg} \approx -\frac{3}{2}n^2J_2\left(\frac{R_e}{r_p}\right)^2 d\Big\{\mathbf{i}_d - 5(\mathbf{i}_{r_p}\cdot\mathbf{i}_d)\mathbf{i}_{r_p} - 5(\mathbf{i}_{r_p}\cdot\mathbf{N})^2\mathbf{i}_d - [10(\mathbf{i}_{r_p}\cdot\mathbf{N})(\mathbf{i}_d\cdot\mathbf{N}) - 35(\mathbf{i}_{r_p}\cdot\mathbf{i}_d)(\mathbf{i}_{r_p}\cdot\mathbf{N})^2]\mathbf{i}_{r_p} + [2(\mathbf{i}_d\cdot\mathbf{N}) - 10(\mathbf{i}_{r_p}\cdot\mathbf{N})(\mathbf{i}_{r_p}\cdot\mathbf{i}_d)]\mathbf{N}\Big\} \tag{30}$$

The total expression for the gravity gradient force is now substituted into equations (21) and (22) to find the even and odd support induced torques. Note that the complete derivation must also consider that r_p is a function of J_2 and e_o as given by equations (5–9). That is, $\mathbf{r}_p$ is written $\mathbf{r}_p(\nu)$.

Odd Harmonic Gyroscope Drift

The odd torque on the gyroscope is computed by substituting the gravity gradient force expressions above into the torque equations and orbit averaging. These are then divided by the angular momentum of the gyroscope and substituted into equation (14) to find the final orbit averaged drift equations due to mass unbalance:

$$\frac{d}{dt}\langle NS\rangle = \frac{z_s}{(2/5)r_g^2\omega_s}\frac{3}{2}dn_o^2\left[\Omega\cos\delta + i'\sin\delta - \frac{EW}{3}\right]$$
$$\frac{d}{dt}\langle EW\rangle = \frac{-z_s}{(2/5)r_g^2\omega_s}\frac{3}{2}dn_o^2\left[\frac{1}{8}J_2\left(\frac{R_e}{r_o}\right)^2\sin 2\delta - \frac{NS}{3}\right] \tag{31}$$

where z_s is the gyroscope mass unbalance along the spin axis, r_g is the gyroscope radius, ω_s is the rotor spin rate, d is the distance from the proof mass to gyroscope center, and n_o is the circular orbit rate $\sqrt{\mu_e/r_o^3}$.

We see that the NS term has the same dependence as the simpler case. However, there is indeed a modification of the EW term due to the Earth oblateness independent of the specified orbit. There is no first order dependence upon the eccentricity. The target orbit must still be chosen, however, to keep the eccentricity small in order to validate the first order assumptions used in the analysis. The target orbit is also chosen to ensure an average co-inclination and node as close to zero as possible over the one year experiment.

Even Harmonic Gyroscope Drift

The even harmonic torques are computed in the same manner. These are significantly more involved, however, as the gravity gradient forces must be expressed in the satellite body-axes, substituted into the quadratic torque expressions, and orbit averaged. While this can be done for the more general even harmonic equations (equations (20)), the resulting drift is dominated by the gyroscope oblateness. It is therefore more straightforward to use the $l = 2$ torque equations (equations (22)). The resulting drifts are given by:

$$\frac{d}{dt}\langle NS\rangle = \frac{-\Delta r\cos\theta_h d^2 n_o^4}{(2/5)r_g^2\omega_s h}\left[\frac{15}{8}(\Omega\cos\delta + i'\sin\delta) - \frac{53}{64}EW + f\left(\frac{n_o}{\beta}\right)\right]$$
$$\frac{d}{dt}\langle EW\rangle = \frac{-\Delta r\cos\theta_h d^2 n_o^4}{(2/5)r_g^2\omega_s h}\left[\frac{33}{32}J_2\left(\frac{R_e}{r_o}\right)^2\sin 2\delta - \frac{1}{64}NS + g\left(\frac{n_o}{\beta}\right)\right] \tag{32}$$

As for the mass unbalance, the NS drift rate is identical to that for a circular orbit about the spherical Earth. However, as in the odd case, the Earth oblateness introduces an EW drift component proportional, in this case, to the sine of twice the guide star declination. There is, again, no first order dependence on the orbit eccentricity.

Note that equations (32) has the additional functions f and g. These functions are nonzero when the roll rate (β) is not an integral multiple of the mean orbit rate (n_o). They arise because some of the terms in the gravity gradient torque that are roll modulated don't exactly average to zero over an orbit unless roll and orbit are

integer multiples. While it is somewhat involved, it is possible to find expressions for these functions. It turns out that the resulting drift is significantly smaller than the leading terms in equations (32), that is, always less than 0.005 milliarcseconds for any combination of roll rates and experiment length.

Direct Gravity Gradient Drift

In addition to the drift mechanism described above, the gyroscopes experience torques due to differences in their moments of inertia interacting with the Earth's gravity gradient. This effect has been known for some time and accounted for in the GP-B error budget. For a spherical Earth, the torque on the gyroscope is given by:

$$\boldsymbol{\tau} = \frac{3\mu_e}{r^3}[\mathbf{i}_r \times (I \cdot \mathbf{i}_r)] \tag{33}$$

where I is the gyroscope inertia tensor and, r the radial position on orbit, $\mathbf{i}_r$ a unit vector along the radius, and μ_e the Earth's gravitational parameter.

In this section we augment equation (33) to consider the torque and resulting drift of the gyroscope for an oblate Earth and averaged over a slightly eccentric orbit. In this case, the torque due to the Earth becomes (again ignoring small terms higher than J_2):

$$\boldsymbol{\tau} = \frac{3\mu_e}{r^3}\left\{\mathbf{i}_r \times (I \cdot \mathbf{i}_r) + \frac{5}{2}J_2\left(\frac{R_e}{r}\right)^2\left[[\mathbf{i}_r \times (I \cdot \mathbf{i}_r)][1 - 7(\mathbf{i}_r \cdot \mathbf{N})^2]\right.\right.$$
$$\left.\left. + 2(\mathbf{i}_r \cdot \mathbf{N})[\mathbf{i}_r \times (I \cdot \mathbf{N}) - (\mathbf{i}_r \cdot I) \times \mathbf{N}] + \frac{2}{5}[(\mathbf{N} \cdot I) \times \mathbf{N}]\right]\right\} \tag{34}$$

The torques on the gyroscope are now computed in the spin axis frame. If we ignore polhoding of the rotor (or average over it) then we can safely approximate the inertia dyadic as diagonal in this frame (that is, assume the spin axis is along the principal axis). This is also a good assumption because a dominant contributor to the inertia difference is the oblateness induced by spin. The resulting inertia matrix is written:

$$I = I_z\begin{bmatrix} 1 - a\varepsilon_o & 0 & 0 \\ 0 & 1 - \varepsilon_o & 0 \\ 0 & 0 & 1 \end{bmatrix} \quad 0 \le a \le 1, \quad \varepsilon_o \approx 5 \times 10^{-6}$$

where ε_o represent the small inertia difference and a allows for an asymmetric rotor. Using this in equation (34) the resulting torque in the spin axis frame is:

$$\tau_1^L \approx \frac{3\mu_e I_z \varepsilon_o}{r^3(\nu)}[-\Omega \cos\nu\cos(\nu-\delta) - i'\sin\nu\cos(\nu-\delta) + EW\cos^2(\nu-\delta)]$$

$$\tau_2^L = \frac{-3\mu_e I_z a\varepsilon_o}{2r^3(\nu)}\left\{\sin(2\nu-2\delta) - NS\cos(2\nu-2\delta) + \frac{5}{2}J_2\left(\frac{R_e}{r(\nu)}\right)^2\left[1 - 7\sin^2\nu\sin(2\nu-2\delta) + 4\sin\nu\cos(\nu-2\delta) + \frac{2}{5}\sin 2\delta\right]\right\} \tag{35}$$

This torque is rotated back into inertial space and inserted into equation (14). It is expanded to first order in J_2 and e_o to find the final orbit averaged drift equations:

$$\frac{d}{dt}\langle NS\rangle = \frac{3}{2}\frac{\varepsilon_o n_o^2}{\omega_s}(-\Omega\cos\delta - i'\sin\delta + EW)$$

$$\frac{d}{dt}\langle EW\rangle = \frac{3}{2}\frac{a\varepsilon_o n_o^2}{\omega_s}\left[\frac{1}{8}J_2\left(\frac{R_e}{r_o}\right)^2\sin 2\delta\right] \tag{36}$$

Sun and Moon Effects

Lastly, it is possible to compute the gravity torques on the gyroscopes due to the Sun and Moon. As before, these fall into both the support dependent and support independent categories. The gravity gradient force on the gyroscope due to a body B a distance $\mathbf{r}_B$ from the center of the Earth is given by:

$$\mathbf{F}_{gg} = -\frac{\mu_B}{|\mathbf{r}_p - \mathbf{r}_B|^3}(\mathbf{r}_p - \mathbf{r}_B) + \frac{\mu_B}{|\mathbf{r}_p - \mathbf{r}_B + \mathbf{d}|^3}(\mathbf{r}_p - \mathbf{r}_B + \mathbf{d}) \tag{37}$$

Assuming r_p/r_B is small, this expression can be expanded to find:

$$\mathbf{F}_{gg} \approx -\frac{\mu_B d}{r_B^3}\left\{3(\mathbf{i}_B\cdot\mathbf{i}_d)\mathbf{i}_B - \mathbf{i}_d + 3\frac{r_p}{r_B}[5(\mathbf{i}_B\cdot\mathbf{i}_d)(\mathbf{i}_B\cdot\mathbf{i}_{r_p})\mathbf{i}_B - (\mathbf{i}_B\cdot\mathbf{i}_d)\mathbf{i}_{r_p} - (\mathbf{i}_{r_p}\cdot\mathbf{i}_d)\mathbf{i}_B - (\mathbf{i}_B\cdot\mathbf{i}_{r_p})\mathbf{i}_d]\right\} \tag{38}$$

This gravity gradient force is then substituted into the support dependent torque equations above in the same way as the Earth torque was computed. In this case, though, it is more complicated because of the complicated time dependence of the Moon's orbit relative to the Sun and Earth. The Sun is more straightforward to orbit average and does result in a closed form solution. For brevity, these results are not shown here. However, both were numerically integrated and found to result in torques at least 3 to 4 orders of magnitude less than the Earth induced drift.

The Sun and Moon also produce a direct gravity gradient torque on the gyroscopes, which to first order is expressed:

$$\boldsymbol{\tau} \approx 3\frac{\mu_B}{r_B^3}\left\{\mathbf{i}_B \times (I \cdot \mathbf{i}_B) + \left(\frac{r_p}{r_B}\right)[-\mathbf{i}_{r_p} \times (I \cdot \mathbf{i}_B) - \mathbf{i}_B \times (I \cdot \mathbf{i}_{r_p}) + 5(\mathbf{i}_{r_p} \cdot \mathbf{i}_B)[\mathbf{i}_B \times (I \cdot \mathbf{i}_B)]]\right\} \tag{39}$$

This torque is negligibly small compared to the others and thus will not be expanded upon here.

Conclusions

This paper examined the torques and resulting drifts on the Gravity Probe B gyroscopes due to gradients in the Earth's gravitational field and due to the influence of the Sun and Moon. While past work has addressed this question, this study expanded it to include the influence of the Earth's oblateness (J_2), an eccentric orbit, and the effect of the Sun and Moon. The results are used for error analysis, data reduction of the flight science data, and for orbit planning. In addition, general equations were presented for the gravity gradient forces and torques on bodies due to the oblate Earth.

The calculations showed a significant contribution to gyroscope drift in the *EW* direction due to the Earth oblateness not realized previously. It was also discovered that gyroscope drift is independent, to first order, of the orbit eccentricity. This is very helpful for final orbit planning as it is very expensive to finely trim the orbit eccentricity.

Table 1 summarizes the critical *EW* drift angle due to Earth oblateness for the baseline GP-B guide star, BH CVn (HR5110), the four current backup stars, and the original GP-B guide star, Rigel. All drift rates fall below the requirement of 0.3 milliarcsec/year. These values were computed for a 2 μin mass unbalance, 2 μin oblateness, and a rotor spinning at 130 Hz. The offset between the gyroscope and drag free sensor is 24.75 cm. A moment of inertia difference ratio for the rotor of 5×10^{-6} was assumed.

TABLE 1. *EW* Gravity Gradient Drift for the GP-B Guide Stars

Star	Declination δ_{2000} (deg)	Frame Dragging (mas/year)	*EW* Gravity Gradient Drift mass unbalance (mas/year)	*EW* Gravity Gradient Drift oblateness (mas/year)	*EW* Direct Gravity Gradient Drift (mas/year)	Total *EW* Gravity Gradient Drift (mas/year)
BH CVn	37.183	33.31	−0.127	−0.103	0.011	−0.230
σ^2 CrB	33.86	34.72	−0.122	−0.099	0.01	−0.221
λ And	46.46	28.8	−0.131	−0.107	0.011	−0.238
V711 Tauri	0.588	41.81	−0.003	−0.002	0	−0.005
IM Peg	16.84	40.02	−0.073	−0.06	0.006	−0.121
Rigel	−8.200	41.4	0.037	0.03	−0.003	0.067

Acknowledgments

This work was performed under NASA contract NAS8-36125.

References

[1] SCHIFF, L. I. "Possible New Experimental Test of General Relativity Theory," *Physical Review Letters,* Vol. 4, No. 5, March 1960, pp. 215–217.

[2] SCHIFF, L. I. "Motion of a Gyroscope According to Einstein's Theory of Gravitation," *Proceedings of the National Academy of Sciences,* Vol. 46, No. 6, June 1960, pp. 871–882.

[3] BARDAS, D., CHEUNG, W. S., GILL, D., HACKER, R., KEISER, G. M., LIPA, J. A., MACGIRVIN, M., SALDINGER, T., TURNEAURE, J. P., WOODING, M. S., and LOCKHART, J. M. "Hardware Development for Gravity Probe-B," in *Cryogenic Optical Systems and Instruments II,* Melugin, R. K. (editor), Proceedings of SPIE, Vol. 619, Bellingham, Washington, 1986, pp. 29–46.

[4] YOUNG, L. S. "Systems Engineering for the Gravity Probe-B Program," in *Cryogenic Optical Systems and Instruments II,* Melugin, R. K. (editor), Proceedings of SPIE, Vol. 619, Bellingham, Washington, 1986, pp. 47–57.

[5] EVERITT, C. W. F., DAVIDSON, D. E., and VAN PATTEN, R. A. "Cryogenic Star-Tracking Telescope for Gravity Probe B," in *Cryogenic Optical Systems and Instruments II,* Melugin, R. K. (editor), Proceedings of SPIE, Vol. 619, Bellingham, Washington, 1986, pp. 89–119.

[6] PARMLEY, R. T., GOODMAN, J., REGELBRUGGE, M., and YUAN, S. "Gravity Probe B Dewar/Probe Concept," in *Cryogenic Optical Systems and Instruments II,* Melugin, R. K. (editor), Proceedings of SPIE, Vol. 619, Bellingham, Washington, 1986, pp. 126–133.

[7] LOCKHART, J. M. "SQUID Readout and Ultra-Low Magnetic Fields for Gravity Probe-B (GP-B)," in *Cryogenic Optical Systems and Instruments II,* Melugin, R. K. (editor), Proceedings of SPIE, Vol. 619, Bellingham, Washington, 1986, pp. 148–156.

[8] VAN PATTEN, R. A., DIESPOSTI, R., and BREAKWELL, J. V. "Ultra High Resolution Science Data Extraction for the Gravity Probe-B Gyro and Telescope," in *Cryogenic Optical Systems and Instruments II,* Melugin, R. K. (editor), Proceedings of SPIE, Vol. 619, Bellingham, Washington, 1986, pp. 157–165.

[9] PARKINSON, B. W., EVERITT, C. W. F., TURNEAURE, J. P., and PARMLEY, R. T. "The Prototype Design of the Stanford Relativity Gyro Experiment," Paper No. IAF-87-458, 38th Congress of the International Astronautical Federation, Brighton, United Kingdom, October 1987.

[10] TURNEAURE, J. P., EVERITT, C. W. F., and PARKINSON, B. W. "The Gravity Probe B Relativity Gyroscope Experiment," in *Proceedings of the Fourth Marcel Grossman Meeting on General Relativity,* Ruffini, P. (editor), Elsevier, New York, 1986, pp. 411–464.

[11] LANGE, B. O. "The Control and Use of Drag-Free Satellites," Ph.D. Dissertation, Department of Aeronautics and Astronautics, Stanford University, Stanford, California, 1964; also "The Drag-Free Satellite," *AIAA Journal,* Vol. 2, No. 9, September 1964, pp. 1590–1606.

[12] KEISER, G. M. "Suspension Torques on a Gimballed Electrostatically Supported Gyroscope and Requirements on the Gyroscopes and Spacecraft for the Relativity Gyroscope Experiment," unpublished report, Hansen Experimental Physics Laboratory, Stanford University, Stanford, California, 1985.

[13] VASSAR, R. "Error Analysis for the Stanford Relativity Gyroscope Experiment," Ph.D. Dissertation, Department of Aeronautics and Astronautics, Stanford University, Stanford, California, 1982.

[14] VASSAR, R., BREAKWELL, J. V., EVERITT, C. W. F., and VAN PATTEN, R. A. "Orbit Selection for the Stanford Relativity Gyroscope Experiment," *Journal of Spacecraft and Rockets,* Vol. 19, No. 1, January-February 1982, pp. 66–71.

[15] AXELRAD, P., VASSAR, R. H., and PARKINSON, B. W. "GP-B Orbit Modeling and Injection Requirements," Paper No. 91-164, AAS/AIAA Spaceflight Mechanics Meeting, Houston, Texas, February 1991.

[16] BREAKWELL, J. V. "Advanced Space Mechanics," Class Notes (AA279B), Department of Aeronautics and Astronautics, Stanford University, Stanford, California.

[17] DiDONNA, B. "Suspension Torque Predictions for the Relativity Gyroscope Experiment," Honors Thesis, Department of Aeronautics and Astronautics, Stanford University, Stanford, California, 1994.

[18] VASSAR, R. "Influence of Proof Mass to Gyro Spacing on Experiment Accuracy," Gravity Probe B Memorandum, LMSC 011/F066213, Lockheed Martin Missiles & Space Company, Palo Alto, California, 1986.